Report

Current Biology

Compact Root Architecture 2 Promotes Root Competence for Nodulation through the miR2111 Systemic Effector

Graphical Abstract

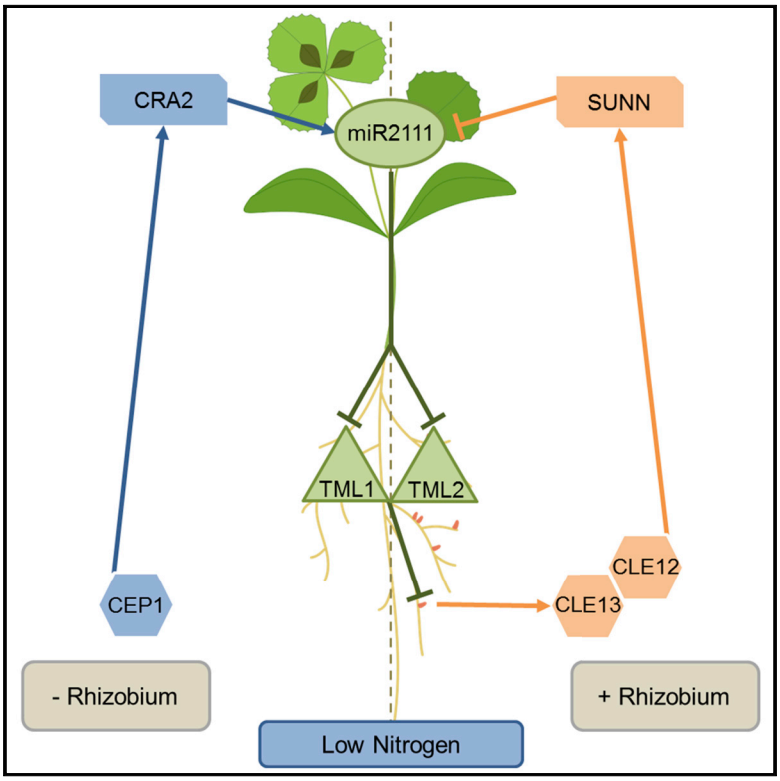

Authors

Pierre Gautrat, Carole Laffont, Florian Frugier

Correspondence

florian.frugier@cnrs.fr

In Brief

Legumes form symbiotic nitrogen-fixing root nodules, whose number is controlled by systemic pathways acting from shoots. Gautrat et al. show that the miR2111 microRNA is a systemic effector acting at the crossroads of the SUNN-negative and CRA2-positive pathways, allowing a dynamic fine-tuning of nodulation by nitrogen and symbiotic rhizobia.

Highlights

- The miR2111 microRNA positively regulates root symbiotic nodulation
- This regulation is systemic from shoots and relies on the CRA2 receptor
- CRA2-related CEP1 peptides and low nitrogen conditions promote miR2111 expression
- The CEP/CRA2 pathway favors root competence to nodulate under low nitrogen

Gautrat et al., 2020, Current Biology *30*, 1339–1345
April 6, 2020
https://doi.org/10.1016/j.cub.2020.01.084

CellPress

Current Biology
Report

Compact Root Architecture 2 Promotes Root Competence for Nodulation through the miR2111 Systemic Effector

Pierre Gautrat,[1] Carole Laffont,[1] and Florian Frugier[1,2,*]
[1]Institute of Plant Sciences – Paris Saclay (IPS2), CNRS, U. Paris-Sud, INRA, U. Paris-Diderot, U. d'Evry, Université Paris-Saclay, Bâtiment 630, rue de Noetzlin, Plateau du Moulon, 91190 Gif-sur-Yvette, France
[2]Lead Contact
*Correspondence: florian.frugier@cnrs.fr
https://doi.org/10.1016/j.cub.2020.01.084

SUMMARY

Nitrogen-deprived legume plants form new root organs, the nodules, following a symbiosis with nitrogen-fixing rhizobial bacteria [1]. Because this interaction is beneficial for the plant but has a high energetic cost, nodulation is tightly controlled by host plants through systemic pathways (acting at long distance) to promote or limit rhizobial infections and nodulation depending on earlier infections and on nitrogen availability [2]. In the *Medicago truncatula* model legume, CLE12 (Clavata3/Embryo surrounding region 12) and CLE13 signaling peptides produced in nodulated roots act in shoots through the SUNN (Super Numeric Nodule) receptor to negatively regulate nodulation and therefore autoregulate nodule number [3–5]. Conversely, CEP (C-terminally Encoded Peptide) signaling peptides produced in nitrogen-starved roots act in shoots through the CRA2 (Compact Root Architecture 2) receptor to promote nodulation already in the absence of rhizobia [6–9]. We show in this study that a downstream shoot-to-root signaling effector of these systemic pathways is the shoot-produced miR2111 microRNA [10] that negatively regulates *TML1* (*Too Much Love 1*) and *TML2* [11] transcripts accumulation in roots, ultimately promoting nodulation. Low nitrogen conditions and CEP1 signaling peptides induce in the absence of rhizobia the production of miR2111 depending on CRA2 activity in shoots, thus favoring root competence for nodulation. Together with the SUNN pathway negatively regulating the same miR2111 systemic effector when roots are nodulated, this allows a dynamic fine-tuning of the nodulation capacity of legume roots by nitrogen availability and rhizobial cues.

RESULTS AND DISCUSSION

Symbiotic nitrogen-fixing nodules form on legume roots when nitrogen is limiting in soils and when compatible bacteria, collectively referred to as rhizobia, are present in the rhizosphere (e.g., *Sinorhizobium medicae* in the case of the *Medicago truncatula* model legume) [12]. These low nitrogen conditions promote the production of CEP (C-terminally Encoded Peptide) signaling peptides in roots [6] that act systemically in shoots through the CRA2 (Compact Root Architecture 2) leucine-rich repeats receptor-like kinase [7–9]. This would lead to the production of shoot-to-root signaling effectors, ensuring the promotion of the root infection by rhizobia to form symbiotic nitrogen-fixing nodules. To explore these yet unknown shoot-to-root signaling effectors recruited downstream of the CEP/CRA2 pathway to promote nodulation under low nitrogen conditions, we analyzed in *M. truncatula* the symbiotic regulation of two previously identified systemic signals: first, CEPD (CEP Downstream) proteins acting as shoot-to-root signaling effectors of the *Arabidopsis thaliana* CRA2 orthologous pathway, CEPR1 (CEP Receptor 1), to promote systemically root nitrogen uptake [13, 14] and, second, the miR2111 microRNA acting in *Lotus japonicus* as a shoot-to-root signaling effector to promote systemically root nodulation [10], which is negatively regulated by the HAR1 (Hypernodulation and Aberrant Root 1) pathway [15, 16] orthologous to SUNN (Super Numeric Nodule) in *M. truncatula* [3].

The Shoot-Produced miR2111 Systemic Signal, but Not MtCEPDs, Is Downregulated in Response to Rhizobium

CEPD proteins most closely related to *Arabidopsis thaliana* proteins were searched in the most recent version of the *M. truncatula* genome (v5; https://medicago.toulouse.inra.fr/MtrunA17r5.0-ANR/) [17] to generate a similarity tree (Figure S1A). Three *M. truncatula* proteins grouped in the same clade as *A. thaliana* CEPD1 and CEPD2 proteins. To determine whether these genes could be functional homologs of *Arabidopsis CEPD* genes and act as systemic effectors, we checked how nitrogen and the CRA2 pathway regulated their expression, using quantitative RT-PCR (qRT-PCR) in wild-type (WT) and *cra2* plants grown with or without NH_4NO_3 5 mM (Figure S1B). In shoots, the expression of two out of the three *MtCEPD* genes, so-called *MtCEPD1* and *MtCEPD2*, was strongly induced by low nitrogen conditions in WT, but not in the *cra2* mutant. This indicates that *MtCEPD1* and *MtCEPD2* regulation by nitrogen relies on the CRA2 receptor, as reported for *AtCEPD1* and *AtCEPD2* genes in *Arabidopsis* [14], suggesting that they are bona fide functional homologs of *Arabidopsis CEPD* genes. In *M. truncatula* roots, the same regulations were however observed, indicating that unlike *Arabidopsis*, *CEPD* genes are

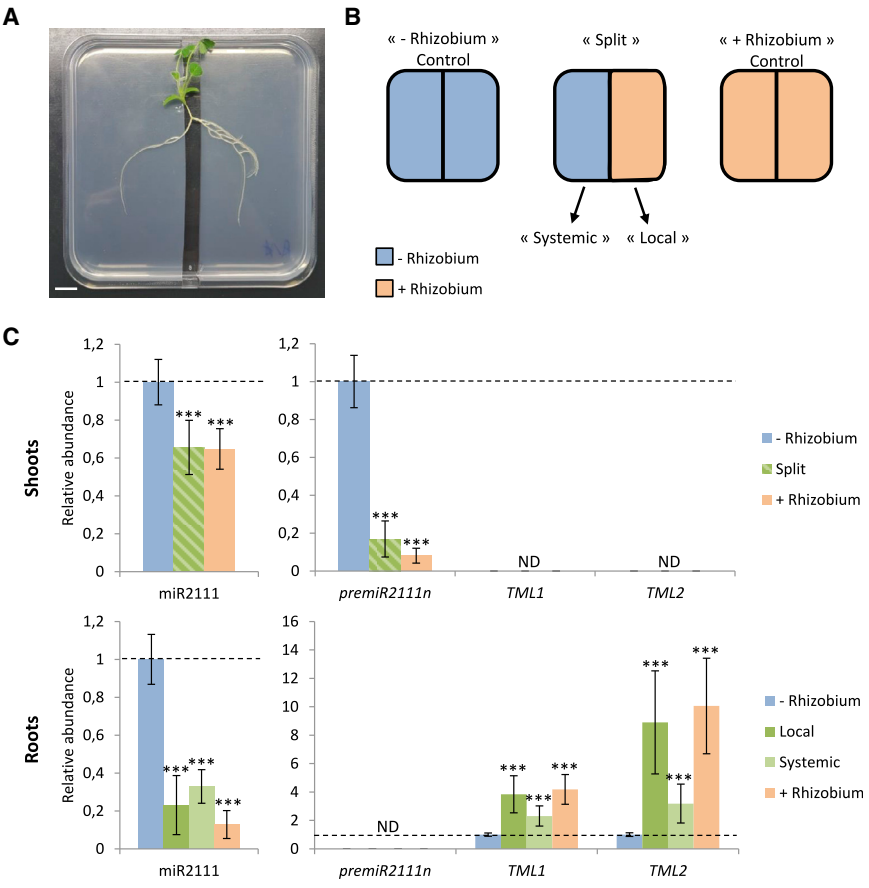

Figure 1. Systemic Accumulation of the miR2111 MicroRNA and of *MtTML* Target Transcripts Is Anti-correlated in Response to Rhizobium

(A) Image of a *M. truncatula* plant growing in an *in vitro* split-root experimental system (scale bar represents 1 cm).

(B) Split-root experimental design with plants either inoculated with rhizobium ("+ Rhizobium" in orange), or not ("− Rhizobium" in blue), or inoculated on only one-half of the root system ("Split" plants, the inoculated side being called "Local" and the non-inoculated side "Systemic").

(C) Transcript levels of *premiR2111n*, *TML1*, and *TML2* genes were analyzed by qRT-PCR and the accumulation of the major miR2111 isoform by stem-loop qRT-PCR in shoots and roots of wild-type (WT) plants grown in the split-root experimental system described in (B), 5 days post-inoculation (5 dpi). Data were normalized to 1 relatively to the non-inoculated control, as indicated with dotted lines. A pool of seven biological replicates (n > 35 plants per condition) is shown, and error bars represent standard deviations. A Student's t test was performed to assess statistical differences with the non-inoculated control (*p < 0.05; **p < 0.001; ***p < 0.0001). ND stands for not detected.

See also Table S1 and Figure S1.

expressed in both shoots and roots and regulated by nitrogen. This implies that *MtCEPD* genes may have local functions to regulate root nitrogen responses. To evaluate a possible link between these nitrogen-regulated *CEPD* genes and symbiotic nodulation, we then tested whether, similarly as previously observed in response to the high nitrogen treatment, their expression was also systemically downregulated after a rhizobium inoculation depending on CRA2. No systemic repression of the expression of these two *MtCEPD* genes was detected in shoots of plants inoculated by rhizobium (Figure S1C). *MtCEPD* genes were even upregulated in response to rhizobium in roots, potentially independently of CRA2, thus showing an antagonistic regulation compared to the high nitrogen treatment. This again suggests that local regulations and functions of *CEPD* genes likely exist in *M. truncatula* roots, which may be different, however, in response to high nitrogen and rhizobium. Overall, *MtCEPD* genes do not appear as clear-cut candidates to mediate a CRA2-dependent systemic regulation of nodulation, even though a complex network of nitrogen- and rhizobium-induced local and systemic regulations may exist.

As an alternative, we analyzed whether the miR2111, recently proposed in *L. japonicus* as a shoot-to-root systemic signal downregulated by rhizobium [10], could be a systemic effector acting downstream of the MtCRA2 pathway. To this aim, we searched for *M. truncatula* miR2111 precursors in the miRbase (http://www.mirbase.org) and MIRMED (https://medicago.toulouse.inra.fr/MIRMEDsolexa.cgi) [18] databases, revealing 18 hits in the genome, all clustered within an ~75-kb region of the chromosome 7 on the reverse strand (Figure S1D; Table S1). In order to identify whether the miR2111 acts as a systemic effector in response to rhizobium, we used a split-root experimental system to separate local from systemic responses. Three conditions were analyzed in parallel: one where one-half of the root system was inoculated or not by rhizobium, defined, respectively, as "Local" versus Systemic" response compartments, and two homogeneous controls where both halves of the split roots were either inoculated ("+ Rhizobium") or not ("− Rhizobium"). Both shoots and roots were analyzed in parallel (Figures 1A and 1B). Among the 18 miR2111 precursors, none was detected by qRT-PCR in WT roots and only six in shoots: the *premiR2111n*, showing the highest expression level; closely followed by the *premiR2111k* and *premiR2111l*; as well as the *premiR2111d*, *premiR2111e*, and *premiR2111q*, having a weaker expression (Figures 1C, displaying the *premiR2111n* as a representative example, and S1E, showing the similar regulation of all other precursors). The 12 other putative miR2111 precursors could not be amplified by qRT-PCR despite designing different primer pairs. After rhizobium inoculation, the expression of the six detectable miR2111 precursors was strongly decreased in shoots and still not detected in roots (Figures 1C and S1E). A stem-loop qRT-PCR analysis was then performed to monitor the mature miR2111 accumulation, which accordingly revealed a decreased accumulation after rhizobium inoculation, not only in shoots but also in each root compartment (local and systemic; Figure 1C). This result is in agreement with *L. japonicus* data and a model where mature microRNAs (miRNAs) move systemically from shoots to roots [10], positioning

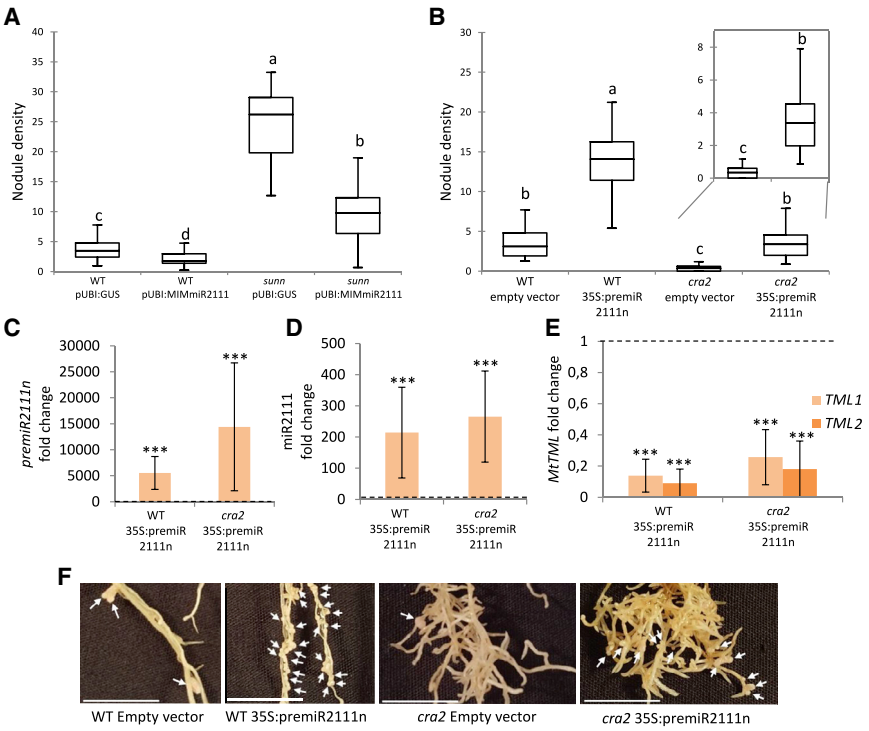

Figure 2. Modulation of miR2111 Accumulation Affects *MtTML* Transcripts Level and Rescues the *sunn* and *cra2* Mutant Nodulation Phenotypes

(A) Nodule density (nodules/mg of root dry weight) of WT and *sunn* mutant roots transformed with a pUBI:*GUS* control vector or a pUBI:*MIMmiR2111* construct, 14 days post-rhizobium inoculation (14 dpi). One representative biological experiment out of three is shown, and a Kruskal-Wallis statistical test was performed to assess significant differences shown by letters ($\alpha < 0.05$; $n > 25$ plants per condition).

(B) Nodule density (nodules/mg of root dry weight) of WT and *cra2* mutant roots transformed with an empty vector or a p35S:*premiR2111n* construct, 14 dpi. One representative biological experiment out of three is shown, and a Kruskal-Wallis statistical test was performed to assess significant differences shown by letters ($\alpha < 0.05$; $n > 20$ plants per condition).

(C–E) The transcript level of the *premiR2111n* (C), the accumulation of the miR2111 (D), and of *TML1* and *TML2* transcripts (E) were analyzed by qRT-PCR in representative roots from three biological replicates (n = 6 plants per condition) grown as described in (B), 5 dpi. Data were normalized to 1 for each genotype relatively to empty vector control roots, as indicated with dotted lines, to highlight the effect of the miR2111 overexpression, and error bars represent standard deviations. A Student's t test was performed to assess statistical differences with the empty vector controls (*$p < 0.05$; **$p < 0.001$; ***$p < 0.0001$).

(F) Details of representative roots analyzed in (B). White arrows indicate nodules (scale bars represent 1 cm).

See also Figure S2.

the miR2111 as an ideal candidate to act as a downstream shoot-to-root systemic effector of the CRA2 pathway.

The miR2111 Regulates *MtTML* Transcripts Level in Roots, and Its Accumulation Is Repressed in Response to Rhizobium through the SUNN Systemic Pathway

In *M. truncatula*, two orthologous *LjTML* genes, *TML1* (*Too Much Love 1*) and *TML2*, encode F-box proteins previously shown to act in roots to negatively regulate nodule number [11, 19, 20]. To determine whether the miR2111 post-transcriptional regulation of *TML* transcripts accumulation in roots is conserved between *L. japonicus* and *M. truncatula* [10], we used two independent already available "degradome" genome-wide datasets [21, 22]. Interestingly, both *MtTML* transcripts were shown to be cleaved by the miR2111 [18] (Figure S2). To independently validate the regulation of *MtTML* transcripts by the miR2111, the *premiR2111n* precursor was overexpressed (p35S:*premiR2111n*; Figure 2C), leading to the accumulation of miR2111 (Figure 2D) and to a reduction of *MtTML* transcripts accumulation (Figure 2E). Conversely, expression of a mimicry construct inhibiting the action of the miRNA (pUBI:*MIMmiR2111*; Figure S2C) showed a reduced accumulation of miR2111 (Figure S2D) and an increased accumulation of *MtTML* transcripts (Figure S2E). Overall, this indicates the functionality of the miR2111, as well as of the *premiR2111n* precursor, to negatively regulate *TML1* and *TML2* transcripts accumulation. These two independent experiments additionally revealed a positive role of the miR2111 on nodule number (Figures 2A, 2B, S2B, and S2G).

We then tested whether *TML1* and *TML2* transcripts accumulation was affected by a rhizobium inoculation using the dedicated split-root experimental system described previously (Figures 1A and 1B). Interestingly, these two validated miR2111 target genes were only detected in roots, and their transcripts accumulated in response to rhizobium either locally or systemically (Figure 1C).

As the miR2111/*MtTML* module was previously associated to the autoregulation of nodulation (AON) pathway in *L. japonicus* [10], we evaluated the conservation of this systemic regulation in *M. truncatula*. To this aim, we analyzed the expression of the miR2111/*MtTML* module in the *sunn* mutant (Figure 3A). The repression of the mature miR2111 accumulation and of miR2111 precursors expression in response to rhizobium was abolished in the *sunn* mutant compared to WT plants (Figures 3A and S3A). Accordingly, the level of *TML1*/*TML2* target transcripts was decreased (Figure 3A). These results established that the regulation by rhizobium of the miR2111/*MtTML* module relies on the SUNN AON pathway in *M. truncatula*.

Compared to data available in *L. japonicus* [10], an additional functional validation was provided to sustain the link between the SUNN/HAR1 pathway and the miR2111/*MtTML* module. The pUBI:*MIMmiR2111* construct inhibiting miR2111 action was expressed in *M. truncatula sunn* mutant roots. The *MIMmiR2111* transgene level correlated with its inhibitory effect on miR2111 accumulation and with an increased *MtTML* transcripts level (Figures S2C–S2E). This miR2111 inhibition was sufficient to rescue the *sunn* mutant supernodulation phenotype, partially

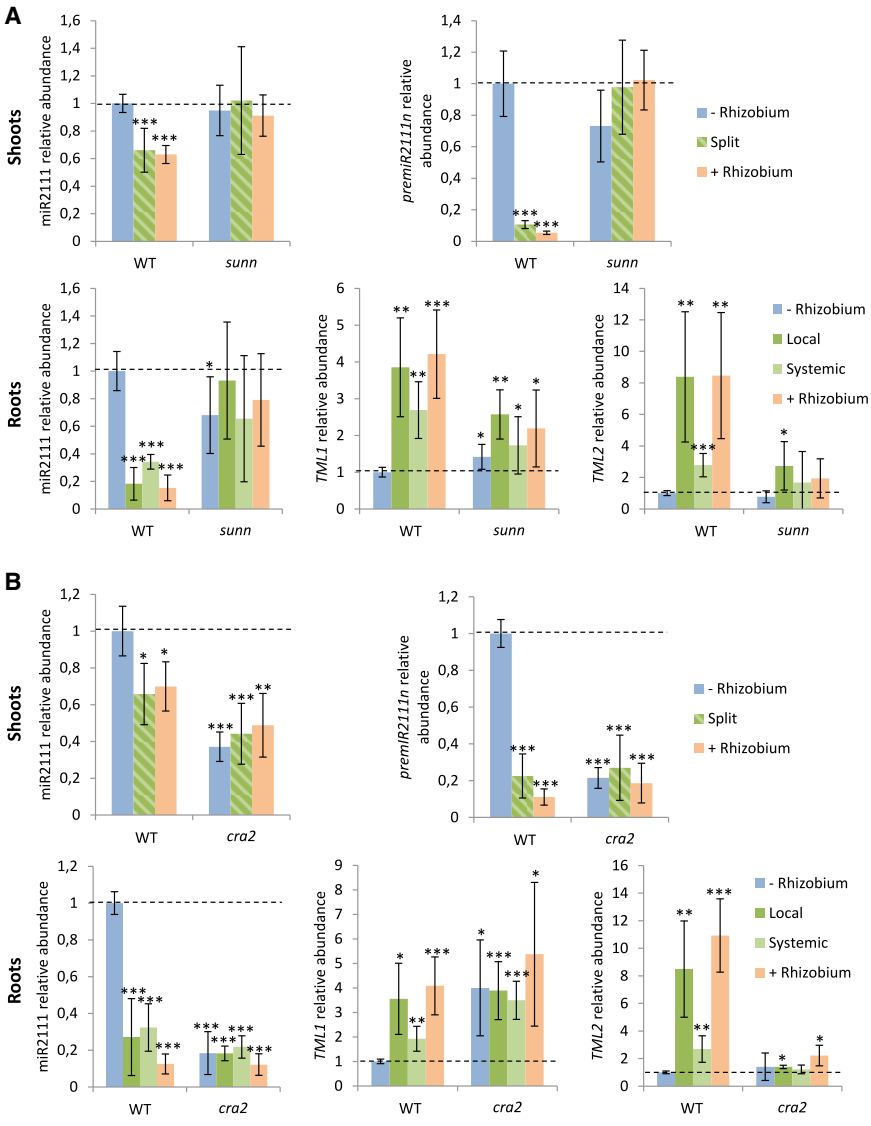

Figure 3. miR2111 Accumulation Is Negatively Regulated by the SUNN Pathway in Response to Rhizobium and Positively by the CRA2 Pathway in the Absence of Rhizobium

(A) Transcript levels of *premiR2111n*, *TML1*, and *TML2* genes were analyzed by qRT-PCR and the accumulation of the major miR2111 isoform by stem-loop qRT-PCR, in shoots and roots of WT and *sunn* mutant plants grown in the split-root experimental system described in Figure 1B, 5 dpi. Data were normalized to 1 relatively to the non-inoculated WT control, as indicated with dotted lines. A pool of three biological replicates (n > 13 plants per conditions) is shown, and error bars represent standard deviations. A Student's t test was performed to assess statistical differences with the non-inoculated WT control (*p < 0.05; **p < 0.001; ***p < 0.0001).

(B) Transcript levels of *premiR2111n*, *TML1*, and *TML2* genes were analyzed by qRT-PCR and the accumulation of the miR2111 by stem-loop qRT-PCR, in shoots and roots of WT and *cra2* mutant plants grown in the split-root experimental system described in Figure 1B, 5 dpi. Data were normalized to 1 relatively to the non-inoculated WT control, as indicated with dotted lines. A pool of three biological replicates (n > 16 plants per condition) is shown, and error bars represent standard deviations between biological replicates. A Student's t test was performed to assess statistical differences with the non-inoculated WT control (*p < 0.05; **p < 0.001; ***p < 0.0001).

See also Figure S3.

when considering nodule density and to a WT level when considering nodule number (Figures 2A, S2B, and S2F).

Overall, these results indicate that the HAR1/SUNN-dependent downregulation of miR2111 expression in shoots challenged with rhizobium is conserved between *L. japonicus* and *M. truncatula* and that impairing miR2111 action is sufficient to rescue the *sunn* supernodulation phenotype.

The CRA2 Receptor Is Required in Shoots to Maintain a High Level of miR2111 Expression in Rhizobial Non-inoculated Plants, Promoting Root Competence to Nodulate

Having validated the miR2111 as a systemic shoot-to-root effector regulating nodule number, we tested whether its accumulation could be promoted by the CRA2 systemic pathway positively regulating nodulation [9]. Strikingly, expression of all miR2111 precursors detectable in shoots and accumulation of the miR2111 in shoots and roots were strongly reduced in the *cra2* mutant already before rhizobium inoculation (Figures 3B and S3B). Accordingly, a higher accumulation of *TML1* target transcripts was detected in *cra2* mutant roots compared to WT plants, even though *TML2* was not deregulated in these experimental conditions (Figure 3B). In response to rhizobium, the low expression and accumulation of the miR2111 was maintained in the *cra2* mutant, and strikingly, miR2111 accumulation in WT rhizobium-inoculated roots was similar to *cra2* non-inoculated roots. This suggests that the *cra2* mutant inability to nodulate [7, 9] may be linked to a basal downregulation of the miR2111 accumulation. In addition, these results demonstrate that the CRA2 systemic pathway is critical to positively regulate miR2111 accumulation in rhizobial non-inoculated plants.

These observations prompted us to test whether an ectopic expression of the miR2111 was sufficient to rescue the *cra2* low-nodulation phenotype. We therefore transformed *cra2* mutant roots with the previously described p35S:*premiR2111n* construct. Overexpression of the *premiR2111n* correlated with an increased miR2111 accumulation and with a decreased *MtTML* transcripts accumulation (Figures 2C–2E). This miR2111 ectopic expression was indeed sufficient to rescue the low *cra2* mutant nodulation phenotype, even at a WT level when the *cra2* compact root phenotype was considered by quantifying the nodule density (Figures 2B, 2F, and S2G).

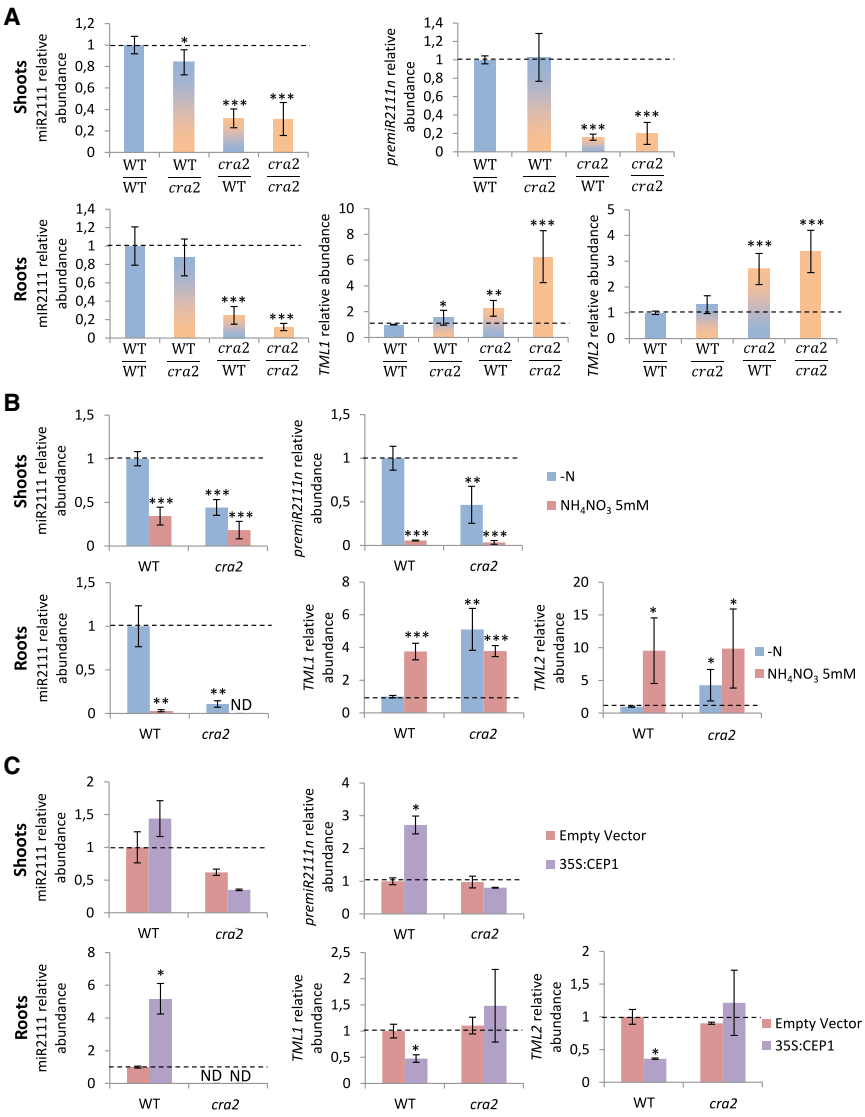

Figure 4. Low Nitrogen and CEP1 Peptides Promote miR2111 Accumulation Depending on the CRA2 Receptor

(A) Transcript levels of *premiR2111n*, *TML1*, and *TML2* genes were analyzed by qRT-PCR and the accumulation of the major miR2111 isoform by stem-loop qRT-PCR, in shoots and roots of grafted WT and *cra2* mutant plants 7 days after transfer on a nitrogen-deprived medium. Data were normalized to 1 relatively to the WT homografted control, as indicated with dotted lines. A pool of three biological replicates (n > 16 plants per condition) is shown, and error bars represent standard deviations between biological replicates. A Student's t test was performed to assess statistical differences with the WT homografted control (*p < 0.05; **p < 0.001; ***p < 0.0001).

(B) Transcripts level of *premiR2111n*, *TML1*, and *TML2* were analyzed by qRT-PCR and accumulation of miR2111 by stem-loop qRT-PCR, in shoots and roots of WT and *cra2* mutant plants 12 days after transfer on a nitrogen-deprived medium (– N) or with nitrogen (+ NH_4NO_3 5 mM). Data were normalized relatively to the nitrogen-deprived WT control, as indicated with dotted lines. A pool of two biological replicates (n > 9 plants per condition) is shown, and error bars represent standard deviations. A Student's t test was performed to assess statistical differences with the nitrogen-deprived WT control (*p < 0.05; **p < 0.001; ***p < 0.0001).

(C) Transcripts level of *premiR2111n*, *TML1*, and *TML2* were analyzed by qRT-PCR and accumulation of miR2111 by stem-loop qRT-PCR, in shoots and roots of WT and *cra2* mutant plants transformed with an empty vector (EV) or a p35S:*CEP1* construct 12 days after transfer on a NH_4NO_3 5 mM medium. Data were normalized relatively to the WT EV control, as indicated with dotted lines. One biological replicate out of two is shown (n > 5 per condition and replicate), and error bars represent standard deviations. A Student's t test was performed to assess statistical differences with the WT EV control (*p < 0.05; **p < 0.001; ***p < 0.0001). See also Figure S4.

As previous grafting studies showed that the CRA2 pathway promotes nodulation from shoots [7, 9], we then tested whether the regulation of the miR2111/*MtTML* module relied on the activity of CRA2 in shoots and/or in roots. Grafts generated between non-inoculated *cra2* and WT plants revealed that the CRA2 activity in shoots, but not in roots, was required to positively regulate *premiR2111n* expression in shoots, as well as miR2111 accumulation in both shoots and roots (Figure 4A). These results are therefore in agreement with previous *cra2* mutant grafting nodulation phenotypes [7, 9]. Interestingly, under these experimental conditions, the accumulation of both *MtTML* transcripts was induced in *cra2* mutant homografted plants. In addition, heterologous grafts revealed that the regulation of *MtTML* transcripts accumulation also relied on the activity of CRA2 in shoots.

Collectively, these results show that the CRA2 pathway positively regulates from shoots miR2111 expression and accumulation. Noteworthy, increasing the accumulation of the miR2111 in the *cra2* mutant was sufficient to rescue its low nodulation phenotype. Overall, this demonstrates that the miR2111/*MtTML* module is a downstream systemic effector of the CRA2 pathway.

Low Nitrogen and CEP1 Signaling Peptides Promote Systemically miR2111 Expression Depending on the CRA2 Receptor

Low nitrogen availability induces in roots the expression of *CEP* peptide encoding genes, such as *CEP1* [6], which act through the CRA2 systemic pathway to stimulate nodulation [8, 9]. To determine whether the miR2111 systemic effector was induced by low nitrogen availability depending on CRA2, we assessed the transcriptional regulation of the miR2111/*MtTML* module in WT and *cra2* mutant plants grown on nitrogen depleted or sufficient conditions (+/– NH_4NO_3 5 mM; Figures 4B and S4A). The expression of miR2111 precursors and the accumulation of miR2111 were higher in the depleted nitrogen condition compared to the high nitrogen condition, and conversely, transcripts accumulation of both *MtTML* genes was decreased, as

expected. In the *cra2* mutant, accumulation of *premiR2111*, miR2111, and *MtTML* transcripts were similar to WT plants grown on high nitrogen, correlating again with the mutant inability to nodulate. These results highlight that the accumulation of the miR2111 systemic effector is promoted by low nitrogen and repressed not only by rhizobium inoculation but also by high nitrogen. In addition, the higher accumulation of miR2111 in nitrogen-starved plants relies on CRA2.

Finally, the role of CEP1 peptides on the regulation of the miR2111 systemic effector was evaluated using an ectopic expression strategy (p35S:*CEP1*) [6] in WT and *cra2* mutant plants (Figures 4C and S4B). *CEP1* transgene overexpression (Figure S4B) promoted the expression of *premiR2111* precursors and miR2111 accumulation, whereas transcripts accumulation of both *MtTML* genes was decreased. In *cra2* mutants, *CEP1* overexpression did not affect the miR2111/*MtTML* module. These results indicate that CEP1 promotes miR2111 accumulation, depending on the CRA2 pathway.

Altogether, we showed that, under low nitrogen conditions, CEP1 signaling peptides act through the CRA2 receptor to promote in shoots the expression of miR2111 precursors, and consequently the accumulation of miR2111 in both shoots and roots, leading to the repression of *MtTML* target transcripts accumulation in roots. As the miR2111 promotes nodulation and can rescue the *cra2* low-nodulation phenotype, this suggests that, under low nitrogen conditions, the CRA2 pathway actively maintains the root competency for nodulation through the downstream miR2111 systemic effector. Together with results obtained in *L. japonicus* [10], our data additionally revealed that the miR2111 systemic effector is at the crossroad of two systemic pathways involving different families of signaling peptides, CLE (Clavata3/Embryo surrounding region) and CEP, which are regulating antagonistically nodulation depending on nitrogen availability and rhizobial cues. The coordination of these two systemic regulatory pathways ultimately ensures a dynamic adaptation of nodule number homeostasis in nutrient heterogeneous and fluctuating environments. Finally, it remains open that *MtCEPD* genes, beside regulating different aspects of root system architecture and nitrate uptake depending on CRA2, as anticipated from the *cra2* "*compact root architecture*" mutant phenotype and as proposed in *Arabidopsis* [13], may also participate in regulating nodulation. If so, *MtCEPD* transcriptional regulations suggest that a combination of local and systemic functions induced in response to nitrogen and/or rhizobium may exist.

STAR★METHODS

Detailed methods are provided in the online version of this paper and include the following:

- KEY RESOURCES TABLE
- LEAD CONTACT AND MATERIALS AVAILABILITY
- EXPERIMENTAL MODEL AND SUBJECT DETAILS
- METHOD DETAILS
  - Cloning procedures and root transformation
  - Long and small RNA extraction and qRT-PCR
  - Similarity tree building
- QUANTIFICATION AND STATISTICAL ANALYSIS
- DATA AND CODE AVAILABILITY

SUPPLEMENTAL INFORMATION

Supplemental Information can be found online at https://doi.org/10.1016/j.cub.2020.01.084.

ACKNOWLEDGMENTS

We thank, at IPS2, Christine Lelandais-Brière for help in using the MIRMED database and fruitful discussions, Hélène Proust for suggestions with small RNA protocols, Corentin Moreau for some primer design, and Ambre Miassod for cheerful help on some experiments and for the graphical abstract drawing. We also thank Pascal Gamas (LIPM, Castanet-Tolosan, France) for sharing preliminary unpublished genomic and transcriptomic analyses that helped the exhaustive identification of premiR2111 loci in the *M. truncatula* genome and Marc Lepetit (LRSV, Montpellier, France) for suggestions on low/high nitrogen conditions to be used. Golden Gate binary vectors were provided by the Engineering Nitrogen Symbiosis for Africa (ENSA) initiative (https://www.ensa.ac.uk/). P.G. was the recipient of a fellowship from the Paris-Sud/Paris-Saclay University. The work was supported by the Agence Nationale de la Recherche (ANR) "PSYCHE" project (ANR-16-CE20-0009-01).

AUTHOR CONTRIBUTIONS

P.G. performed most of the experiments, with help from C.L. F.F. conceived the project. P.G. and F.F. wrote the manuscript.

DECLARATION OF INTERESTS

The authors declare no competing interests.

Received: August 28, 2019
Revised: December 11, 2019
Accepted: January 29, 2020
Published: February 27, 2020

REFERENCES

1. Suzaki, T., Yoro, E., and Kawaguchi, M. (2015). Leguminous plants: inventors of root nodules to accommodate symbiotic bacteria. Int. Rev. Cell Mol. Biol. *316*, 111–158.
2. Okamoto, S., Tabata, R., and Matsubayashi, Y. (2016). Long-distance peptide signaling essential for nutrient homeostasis in plants. Curr. Opin. Plant Biol. *34*, 35–40.
3. Schnabel, E., Journet, E.P., de Carvalho-Niebel, F., Duc, G., and Frugoli, J. (2005). The *Medicago truncatula* SUNN gene encodes a CLV1-like leucine-rich repeat receptor kinase that regulates nodule number and root length. Plant Mol. Biol. *58*, 809–822.
4. Mortier, V., Den Herder, G., Whitford, R., Van de Velde, W., Rombauts, S., D'Haeseleer, K., Holsters, M., and Goormachtig, S. (2010). CLE peptides control *Medicago truncatula* nodulation locally and systemically. Plant Physiol. *153*, 222–237.
5. Mortier, V., De Wever, E., Vuylsteke, M., Holsters, M., and Goormachtig, S. (2012). Nodule numbers are governed by interaction between CLE peptides and cytokinin signaling. Plant J. *70*, 367–376.
6. Imin, N., Mohd-Radzman, N.A., Ogilvie, H.A., and Djordjevic, M.A. (2013). The peptide-encoding CEP1 gene modulates lateral root and nodule numbers in *Medicago truncatula*. J. Exp. Bot. *64*, 5395–5409.
7. Huault, E., Laffont, C., Wen, J., Mysore, K.S., Ratet, P., Duc, G., and Frugier, F. (2014). Local and systemic regulation of plant root system architecture and symbiotic nodulation by a receptor-like kinase. PLoS Genet. *10*, e1004891.
8. Mohd-Radzman, N.A., Laffont, C., Ivanovici, A., Patel, N., Reid, D., Stougaard, J., Frugier, F., Imin, N., and Djordjevic, M.A. (2016). Different pathways act downstream of the CEP peptide receptor CRA2 to regulate lateral root and nodule development. Plant Physiol. *171*, 2536–2548.

9. Laffont, C., Huault, E., Gautrat, P., Endre, G., Kalo, P., Bourion, V., Duc, G., and Frugier, F. (2019). Independent regulation of symbiotic nodulation by the SUNN negative and CRA2 positive systemic pathways. Plant Physiol. *180*, 559–570.
10. Tsikou, D., Yan, Z., Holt, D.B., Abel, N.B., Reid, D.E., Madsen, L.H., Bhasin, H., Sexauer, M., Stougaard, J., and Markmann, K. (2018). Systemic control of legume susceptibility to rhizobial infection by a mobile microRNA. Science *362*, 233–236.
11. Gautrat, P., Mortier, V., Laffont, C., De Keyser, A., Fromentin, J., Frugier, F., and Goormachtig, S. (2019). Unraveling new molecular players involved in the autoregulation of nodulation in *Medicago truncatula*. J. Exp. Bot. *70*, 1407–1417.
12. Oldroyd, G.E.D. (2013). Speak, friend, and enter: signalling systems that promote beneficial symbiotic associations in plants. Nat. Rev. Microbiol. *11*, 252–263.
13. Tabata, R., Sumida, K., Yoshii, T., Ohyama, K., Shinohara, H., and Matsubayashi, Y. (2014). Perception of root-derived peptides by shoot LRR-RKs mediates systemic N-demand signaling. Science *346*, 343–346.
14. Ohkubo, Y., Tanaka, M., Tabata, R., Ogawa-Ohnishi, M., and Matsubayashi, Y. (2017). Shoot-to-root mobile polypeptides involved in systemic regulation of nitrogen acquisition. Nat. Plants *3*, 17029.
15. Wopereis, J., Pajuelo, E., Dazzo, F.B., Jiang, Q., Gresshoff, P.M., De Bruijn, F.J., Stougaard, J., and Szczyglowski, K. (2000). Short root mutant of *Lotus japonicus* with a dramatically altered symbiotic phenotype. Plant J. *23*, 97–114.
16. Nishimura, R., Hayashi, M., Wu, G.J., Kouchi, H., Imaizumi-Anraku, H., Murakami, Y., Kawasaki, S., Akao, S., Ohmori, M., Nagasawa, M., et al. (2002). HAR1 mediates systemic regulation of symbiotic organ development. Nature *420*, 426–429.
17. Pecrix, Y., Staton, S.E., Sallet, E., Lelandais-Brière, C., Moreau, S., Carrère, S., Blein, T., Jardinaud, M.F., Latrasse, D., Zouine, M., et al. (2018). Whole-genome landscape of *Medicago truncatula* symbiotic genes. Nat. Plants *4*, 1017–1025.
18. Formey, D., Sallet, E., Lelandais-Brière, C., Ben, C., Bustos-Sanmamed, P., Niebel, A., Frugier, F., Combier, J.P., Debellé, F., Hartmann, C., et al. (2014). The small RNA diversity from *Medicago truncatula* roots under biotic interactions evidences the environmental plasticity of the miRNAome. Genome Biol. *15*, 457.
19. Magori, S., Oka-Kira, E., Shibata, S., Umehara, Y., Kouchi, H., Hase, Y., Tanaka, A., Sato, S., Tabata, S., and Kawaguchi, M. (2009). Too much love, a root regulator associated with the long-distance control of nodulation in *Lotus japonicus*. Mol. Plant Microbe Interact. *22*, 259–268.
20. Takahara, M., Magori, S., Soyano, T., Okamoto, S., Yoshida, C., Yano, K., Sato, S., Tabata, S., Yamaguchi, K., Shigenobu, S., et al. (2013). Too much love, a novel Kelch repeat-containing F-box protein, functions in the long-distance regulation of the legume-Rhizobium symbiosis. Plant Cell Physiol. *54*, 433–447.
21. Devers, E.A., Branscheid, A., May, P., and Krajinski, F. (2011). Stars and symbiosis: microRNA- and microRNA*-mediated transcript cleavage involved in arbuscular mycorrhizal symbiosis. Plant Physiol. *156*, 1990–2010.
22. Zhou, Z.S., Zeng, H.Q., Liu, Z.P., and Yang, Z.M. (2012). Genome-wide identification of Medicago truncatula microRNAs and their targets reveals their differential regulation by heavy metal. Plant Cell Environ. *35*, 86–99.
23. Terpolilli, J.J., O'Hara, G.W., Tiwari, R.P., Dilworth, M.J., and Howieson, J.G. (2008). The model legume *Medicago truncatula* A17 is poorly matched for N_2 fixation with the sequenced microsymbiont *Sinorhizobium meliloti* 1021. New Phytol. *179*, 62–66.
24. Boisson-Dernier, A., Chabaud, M., Garcia, F., Bécard, G., Rosenberg, C., and Barker, D.G. (2001). Agrobacterium rhizogenes-transformed roots of *Medicago truncatula* for the study of nitrogen-fixing and endomycorrhizal symbiotic associations. Mol. Plant Microbe Interact. *14*, 695–700.
25. Frugier, F., Poirier, S., Satiat-Jeunemaître, B., Kondorosi, A., and Crespi, M. (2000). A Krüppel-like zinc finger protein is involved in nitrogen-fixing root nodule organogenesis. Genes Dev. *14*, 475–482.
26. Karimi, M., Inzé, D., and Depicker, A. (2002). GATEWAY vectors for Agrobacterium-mediated plant transformation. Trends Plant Sci. *7*, 193–195.
27. Gouy, M., Guindon, S., and Gascuel, O. (2010). SeaView version 4: A multiplatform graphical user interface for sequence alignment and phylogenetic tree building. Mol. Biol. Evol. *27*, 221–224.
28. Fahraeus, G. (1957). The infection of clover root hairs by nodule bacteria studied by a simple glass slide technique. J. Gen. Microbiol. *16*, 374–381.
29. Blondon, F. (1964). Contribution à l'étude du développement des graminées fourragères ray-grass et dactyle. PhD thesis (University of Paris).
30. Weber, E., Engler, C., Gruetzner, R., Werner, S., and Marillonnet, S. (2011). A modular cloning system for standardized assembly of multigene constructs. PLoS ONE *6*, e16765.
31. Proust, H., Bazin, J., Sorin, C., Hartmann, C., Crespi, M., and Lelandais-Brière, C. (2018). Stable inactivation of microRNAs in *Medicago truncatula* roots. In Functional Genomics in Medicago truncatula. Methods in Molecular Biology, L. Cañas, and J. Beltrán, eds. (Humana), pp. 123–132.
32. Lelandais-Brière, C., Naya, L., Sallet, E., Calenge, F., Frugier, F., Hartmann, C., Gouzy, J., and Crespi, M. (2009). Genome-wide *Medicago truncatula* small RNA analysis revealed novel microRNAs and isoforms differentially regulated in roots and nodules. Plant Cell *21*, 2780–2796.

STAR★METHODS

KEY RESOURCES TABLE

REAGENT or RESOURCE	SOURCE	IDENTIFIER
Bacterial Strains		
Sinorhizobium meliloti Sm1021	[23]	Lab#Sm1021
Sinorhizobium medicae WSM419	[23]	Lab#WSM419
Escherichia coli DH5α	ThermoFisher Scientific https://www.thermofisher.com	Cat#18258012
Agrobacterium rhizogenes Arqua1	[24]	Lab#Arqua1
Critical Commercial Assays		
mirVana miRNA isolation kit	ThermoFisher Scientific https://www.thermofisher.com	Cat#AM1560
Quick-RNA Miniprep Kit	Zymo Research https://www.zymoresearch.com	Cat#R1055
SuperScript III Reverse Transcriptase	ThermoFisher Scientific https://www.thermofisher.com	Cat#18080044
LightCycler 480 SYBR Green I Master	Roche https://lifescience.roche.com	Cat#04887352001
Experimental Models: Organisms		
Medicago truncatula A17	[17]	Lab#MtJemA17
Medicago truncatula sunn-4	[3]	Lab#MtJem*sunn-4*
Medicago truncatula cra2-11	[9]	Lab#MtJem*cra2-11*
Oligonucleotides		
Listed in Table S2	Eurofins https://www.eurofinsgenomics.eu/	Oligos IDs listed in Table S2
Recombinant DNA		
pUBI:*GUS*	This manuscript	Lab#GG-OEGUS
pUBI:*MIMmiR2111*	This manuscript	Lab#GG-MIMmiR2111
pMF2 Empty Vector	[25]	Lab#pMF2
p35S:*premiR2111n*	This manuscript	Lab#pMF2-OEpremiR2111n
pK7WG2D Empty vector	[26]	Lab#pK7WG2D-empty
p35S:*CEP1*	[6]	Lab#pK7WG2D-OECEP1
Softwares		
XLSTAT	https://www.xlstat.com/	Xlstat-Basic-v17.06
SeaView4	[27] http://doua.prabi.fr/software/seaview	SeaView-v4.6.1

LEAD CONTACT AND MATERIALS AVAILABILITY

Further information and requests for resources and reagents should be directed to and will be fulfilled by the Lead Contact, Florian Frugier (florian.frugier@cnrs.fr).

All unique/stable reagents generated in this study (p35S:*premiR2111n*, pUBI:*GUS* and pUBI:*MIMmiR2111* constructs) are available from the Lead Contact with a completed Materials Transfer Agreement.

EXPERIMENTAL MODEL AND SUBJECT DETAILS

The *Medicago truncatula* Jemalong A17 wild-type genotype, as well as the *cra2-11* mutant that contains an insertion in the region encoding the kinase domain (Key Resources Table), and the *sunn-4* mutant that has a mutation introducing a stop codon at the residue 58 (Key Resources Table), were used in this study. Seeds were scarified for 3 minutes using pure sulfuric acid (Sigma), washed four times with water and sterilized for 20 minutes with Bayrochlore (3.75 g/L, Bayrol, Chlorofix). Seeds were then washed again, transferred onto a water/BactoAgar plate (Sigma), stratified for four days in the dark at 4°C, and then germinated at 24°C in the dark for one night.

For *in vitro* split-root and grafting experiments, seedlings were placed onto a growth culture paper (Mega International, https://mega-international.com/) in vertical 1,5% BactoAgar plates containing Fahraeus medium [28] (0.132 g/L $CaCl_2$, 0.12 g/L $MgSO_4.7H_2O$, 0.1 g/L KH_2PO_4, 0.075 g/L $Na_2HPO_4.2H_2O$, 5 mg/L Fe-citrate, and 0.07 mg/L each of $MnCl_2.4H_2O$, $CuSO_4.5H_2O$, $ZnCl_2$, H_3BO_3, and $Na_2MoO_4.2H_2O$) with nitrogen (1mM NH_4NO_3, F+), in a growth chamber with a 16h photoperiod, a light intensity of 150μE, and a temperature of 24°C. For split-root experiments, roots were then cut five days post-germination (dpg), seedlings were grown in between two growth papers for one week, and an additional week without growth paper. Plants with two equivalent

roots were then selected and transferred onto Fahraeus medium without nitrogen (F-) on a plate where the agar was separated in two halves. For grafting experiments, roots were cut from shoots also at five dpg and grafts were generated by cutting plants hypocotyls and reassembling roots and shoots of appropriate genotypes together within a capillary tube, as described in [9] and in the *M. truncatula* handbook (chapter Cuttings and Grafts; http://www.noble.org/medicagohandbook/). After two weeks, grafted plants were transferred onto F- medium plates.

For composite plants experiments (see Method Details), plants were transferred *in vitro* on an F medium with or without NH_4NO_3 5mM, for high/low nitrogen experiments; and on an F medium with NH_4NO_3 5mM for the CEP1 overexpression experiment. For composite plant nodulation experiments, plants were transferred into a pot containing a sand:perlite 1:3 mixture and placed in a growth chamber with a 16h photoperiod, a light intensity of 150µE, a temperature of 24°C, and 65% of relative humidity. Plants were watered with an ''i'' growth medium with low nitrogen (KNO_3 0.25mM) [29]. Stock solution of this medium is obtained by mixing 250mL of each of the following components: KNO_3 20,2g/L, KH_2PO_4 27,2g/L, $CaCl_2$ ($2H_2O$) 73 g/L, $MgSO_4$ ($7H_2O$) 24,6g/L, K_2SO_4 43,5g/L, $EDTA_2Na_2Fe$ 8,2g/L. 13,5mL of the following mix is then added: H_3BO_3 11 g/L, $MnSO_4$ 6,2g/L, KCl 10 g/L, $ZnSO_4$ ($7H_2O$) 1g/L, $(NH_4)6Mo_7O_{24}$ ($4H_2O$) 1g/L, $CuSO_4$ ($5H_2O$) 0.5g/L, H_2SO_4 95% 0.5mL.This stock solution is diluted 40 times with deionized water before use.

Two different strains of rhizobium were used in this study: *Sinorhizobium meliloti* 1021 (Key Resources Table) for early stage nodulation *in vitro* experiments, and *Sinorhizobium medicae* WSM419 (Key Resources Table) for late stage nodulation experiments in pots. Both strains were grown for 24 hours at 30°C in a Yeast Broth Extract medium (YEB), supplemented with 100µg/ml streptomycin (Sigma) or 50µg/mL chloramphenicol (Sigma) for the Sm1021 or the WSM419 strain, respectively. Rhizobium inoculations were performed using an overnight grown bacterial culture diluted at an OD_{600nm} = 0.05 for pots and at an OD_{600nm} = 0.2 for *in vitro* split-root experiments. Composite and split-root plants were inoculated with rhizobium seven days after transfer to pots and to F- plates, respectively. Nodule number and root dry weight were measured at 14 days post rhizobium inoculation (dpi).

METHOD DETAILS

Cloning procedures and root transformation

The pUBI:*MIMmiR2111* (Key Resources Table) construct was generated using Golden Gate cloning [30] and a synthetic MIMmiR2111 gene (Twist Bioscience, http://www.twistbioscience.com/; sequence indicated in the Table S2) as described in [31] in the EC50507 binary vector (https://www.ensa.ac.uk/). A pUBI:*GUS* control vector was also generated using the same strategy in the same binary vector.

The p35S:*premiR2111n* (Key Resources Table) construct was obtained by restriction cloning using the binary vector pMF2 (Key Resources Table). The *premiR2111n* gene was amplified from *M. truncatula* A17 genomic DNA by Polymerase Chain Reaction (PCR) using forward and reverse primers flanked by BamHI and EcoRI restriction sites, respectively (the list of primers used is given in the Table S2). The *premiR2111n* PCR amplicon was then integrated into the pMF2 vector downstream of a 35S:CaMV (Cauliflower Mosaic Virus) cassette using these restriction sites. The p35S:*CEP1* construct was generated in [6] (Key Resources Table).

Clonings were generated using thermocompetent DH5α *Escherichia coli* (Key Resources Table), and final binary vectors used for plant transgenesis were transformed into *Agrobacterium rhizogenes* Arqua1 (Key Resources Table).

''Composite plants'' were obtained *in vitro* by cutting germinated seedling roots and dipping the root sections into a bacterial mat of the *A. rhizogenes* Arqua1 strain containing the construct of interest, as described in [24], followed by two weeks of kanamycin selection (25µg/mL) on a F+ medium.

Long and small RNA extraction and qRT-PCR

Total RNAs were extracted using the miRvana kit (Key Resources Table) or the Quick-RNA Miniprep kit (Key Resources Table), from non-inoculated or five dpi plants for split-roots, from non-inoculated plants for the MIMmiR2111, from 12 days after transfer (corresponding to five dpi) for miR2111 overexpression experiments, from seven days after transfer on the F- medium for grafts, and from 12 days after transfer for nitrogen response and CEP1 overexpression experiments. RNAs were then treated with a DNase1 RNase-free (Thermofisher) following manufacturer instructions. cDNAs were obtained using the SuperScript III Reverse Transcriptase (200U/µL, Key Resources Table) following manufacturer instructions. A stem-loop Reverse Transcription (RT) was performed to amplify each specific mature miRNA by including amplification adapters (listed in the Table S2) to the RT mix, as described in [31]. Two independent cDNA samples were generated from each RNA sample as technical replicates.

Gene expression was analyzed by quantitative RT-PCR (qRT-PCR) on a LightCycler480 apparatus (Roche) using the Light Cycler 480 SYBR Green I Master mix (Key Resources Table) and dedicated specific primers to amplify genes of interest (listed in the Table S2). Forty amplification cycles (15 s at 95°C, 15 s at 60°C, 15 s at 72°C) were performed, as well as a final fusion curve from 60 to 95°C to assess primers specificity. Amplicons were independently sequenced to confirm their specificity. Primer efficiency was systematically tested and only primers with efficiency over 90% were retained. Gene expression was normalized using two different reference genes, *MtActin11* and *MtRNA Binding Protein 1* (*MtRBP1*), while miRNA accumulation was normalized using the miR162 mature miRNA and the U6 small nuclear RNA [32]. In figures, *MtActin11* and miR162 references were selected to normalize the data.

Similarity tree building

The similarity tree was built using the Seaview4 software (Key Resources Table). Proteins were aligned with MUSCLE, alignments were optimized with Gblocks, and the tree was generated based on the bootstrap method (1000 replicates).

QUANTIFICATION AND STATISTICAL ANALYSIS

Statistical analyses were performed with the XLSTAT software (Key Resources Table) using Kruskal-Wallis tests for phenotyping experiments and Student t tests for qRT-PCR experiments. Results of statistical tests are represented by letters or stars in Figures. Specificities of each test and of graphical representations are mentioned in each Figure legend and below: n represents the number of plants analyzed; for qRT-PCR data, means and standard deviations (SD) are shown, and for plant phenotyping, medians and quartiles are shown. Statistical significance was defined as follows: $\alpha < 0.05$ for Kruskal-Wallis tests; and *, $p < 0.05$, **, $p < 0.001$, and ***, $p < 0.0001$ for Student t tests. No data were excluded in this study.

DATA AND CODE AVAILABILITY

The datasets supporting the current study have not been deposited in any public repository but are available from the Lead Contact upon request.